

The Pairing Probability of Massive Black Holes in Merger Galaxies in the Presence of Radiative Feedback

KUNYANG LI,¹ TAMARA BOGDANOVIĆ,¹ AND DAVID R. BALLANTYNE¹

¹*School of Physics and Center for Relativistic Astrophysics, 837 State St NW, Georgia Institute of Technology, Atlanta, GA 30332, USA*

ABSTRACT

Dynamical friction (DF) against stars and gas is thought to be an important mechanism for orbital evolution of massive black holes (MBHs) in merger remnant galaxies. Recent theoretical investigations however show that DF does not always lead to MBH inspiral. For MBHs evolving in gas-rich backgrounds, the ionizing radiation that emerges from the innermost parts of their accretion flow can affect the surrounding gas in such a way to cause the MBHs to accelerate and gain orbital energy. This effect was dubbed “negative DF”. We use a semi-analytic model to study the impact of negative DF on pairs of MBHs in merger remnant galaxies evolving under the combined influence of stellar and gaseous DF. Our results show that for a wide range of merger galaxy and MBH properties negative DF reduces the MBH pairing probability by $\sim 46\%$. The suppression of MBH pairing is most severe in galaxies with one or more of these properties: (1) a gas fraction of $f_g \geq 0.1$; (2) a galactic gas disk rotating close to the circular velocity; (3) MBH pairs in prograde, low eccentricity orbits, and (4) MBH pairs with mass $< 10^8 M_\odot$. The last point is of importance because MBH pairs in this mass range are direct progenitors of merging binaries targeted by the future space-based gravitational wave observatory LISA.

Keywords: Dynamical friction (442) — Galaxy dynamics (591) — Galaxy evolution (594) — Galaxy mergers (608) — Supermassive black holes (1663)

1. INTRODUCTION

Massive black holes (MBHs), with masses in the range $\sim 10^6 - 10^{10} M_\odot$, are known to exist in the centers of most galaxies (Soltan 1982; Kormendy & Richstone 1995; Magorian et al. 1998). After two galaxies merge, a MBH pair¹ may inspiral in the remnant galaxy and coalesce due to the emission of gravitational waves (GWs; Begelman et al. 1980). At separations of ~ 1 kpc, the orbital decay of MBHs is expected to be driven by dynamical friction (DF) by stars and gas (Chandrasekhar 1943; Ostriker 1999) in the remnant galaxy. The evolution timescale of such pairs to separations where they form gravitationally bound binaries is determined by the properties of the two MBHs and their host galaxy.

In earlier work (Li et al. 2020, hereafter LBB20), we found that the percentage of MBHs that form gravitationally bound binaries within a Hubble time is $> 80\%$ in remnant galaxies with gas fractions $< 20\%$, and in galaxies hosting MBH pairs with total mass $> 10^6 M_\odot$ and mass ratios $\gtrsim 1/4$.

Among these, the remnant galaxies with the fastest formation of MBHBs have at least one of these properties: large stellar bulge, comparable mass MBHs, and a galactic gas disk rotating close to the circular velocity. In such galaxies, the MBHs with the shortest inspiral times are either on circular prograde orbits or on very eccentric retrograde orbits. These MBHs are the most likely progenitors of coalescing binaries, whose GWs are expected to be detected by the pulsar timing arrays (PTAs; Foster & Backer 1990; Shannon et al. 2015; Lentati et al. 2015; Arzoumanian et al. 2018) and the Laser Interferometer Space Antenna (LISA; Amaro-Seoane et al. 2017; Klein et al. 2016a) in the next few to 15 years.

Inspiral and coalescence of MBH pairs within a Hubble time is not a inevitable, even when merger galaxies and their MBHs have the properties described above. For example, it was recently shown for MBHs evolving in gas-rich backgrounds that ionizing radiation emerging from the innermost parts of the MBHs’ accretion flows can affect their gaseous DF wake and render gas DF inefficient for a range of physical scenarios. MBHs in this regime tend to experience positive net force, meaning that they speed up, contrary to the expectations for gaseous DF without radiative feedback (Park & Bogdanović 2017; Gruzinov et al. 2020; Toyouchi et al. 2020). This effect, dubbed “negative DF”, is only present when the system satisfies the following criteria (Inayoshi et al. 2016; Park & Bogdanović 2017):

$$(1 + \mathcal{M}^2)M_{\text{bh}}n_\infty < 10^9 M_\odot \text{ cm}^{-3} T_4^{1.5}, \mathcal{M} < 4 \quad (1)$$

¹ We refer to the system of two MBHs as a MBH pair when they are not gravitationally bound, and as a MBH binary (MBHB) when they are gravitationally bound.

Table 1. Galaxy Model Parameters

Symbol	Description	Values
M_{bin}	total MBH pair mass	$(2, 3, 5) \times 10^5 M_{\odot}$ $(1, 3) \times 10^6 M_{\odot}$ $(1, 3) \times 10^7 M_{\odot}$ $(1, 3) \times 10^8 M_{\odot}$
q	MBH mass ratio	$1/n$ ($n = 2, \dots, 9$)
$n_{\text{gd}0}$	central gas number density	100, 200, 300 cm^{-3}
f_{gd}	gas disk mass fraction	0.3, 0.5, 0.9
$v_{\text{g}}(r)$	gas disk rotational speed in steps of $0.1v_{\text{c}}(r)$	$-0.9v_{\text{c}}(r), \dots, 0.9v_{\text{c}}(r)$

NOTE— $v_{\text{g}} > 0$ ($v_{\text{g}} < 0$) corresponds to the sMBH corrotating (counterrotating) with the galactic disk.

where M_{bh} is the mass of the orbiting MBH, n_{∞} is the gas number density “at infinity”, unaffected by the gravity of the MBH, and $T_4 = T/10^4$ K is the gas temperature at the position of the orbiting MBH. Here, $\mathcal{M} = \Delta v/c_s$ is the Mach number, Δv is the speed of the MBH relative to the gas, $c_s = \sqrt{5kT/3m_{\text{p}}}$ is the sound speed, and other constants have their usual meaning.

The first criterion in equation 1 provides a limit within which the size of the ionized region around the MBH is larger than its trailing gaseous DF wake, and so the ionizing radiation suppresses its formation. Without the dense trailing wake, the MBH is pulled “forward” and accelerated by the dense shell of gas that forms in front of the MBH due to the “snowplow” effect caused by radiation pressure (Park & Bogdanović 2017).

However, MBHs under the influence of negative DF do not perpetually accelerate. According to the second criterion, which follows directly from the jump conditions for ionization fronts (Park & Ricotti 2013), a limit exists for the maximum MBH velocity that can be achieved due to negative DF. This limit suggests that, without any other external forces, MBHs that are subject to negative DF should move with an equilibrium $\mathcal{M} \sim \text{few}$. MBHs that do not satisfy these criteria, either because their speed corresponds to $\mathcal{M} \gtrsim 4$, or because they are embedded in sufficiently high density gas, are subject to classical gaseous DF described by Ostriker (1999).

If prevalent in real merger galaxies, negative gaseous DF can lengthen the inspiral time of MBHs. Its implications for the formation and coalescence rate of MBHBs in galactic and cosmological settings are however yet to be understood. Our work is an extension of earlier studies that employed N-body simulations of MBH pairs in stellar environments (Quinlan 1996; Quinlan & Hernquist 1997; Yu 2002; Berczik et al. 2006; Khan et al. 2011, 2013, and others), hydrodynamic simulations of MBH pairs in gas-rich environments (Escala et al. 2005; Dotti et al. 2007; Cuadra et al. 2009), and semi-analytic models of MBH orbital decay (Antonini & Merritt 2012; Barausse 2012; Klein et al. 2016b; Berti et al. 2016;

Dosopoulou & Antonini 2017; Kelley et al. 2017a,c). Here, we consider the DF from both stars and gas in the galaxy, and, for the first time, quantify the effect of negative gaseous DF on the inspiral time and pairing probability of MBHBs.

2. METHODS

In this work we build upon a semi-analytic model presented by LBB20, which describes the orbital evolution of MBH pairs under the influence of stellar and gaseous DF without radiative feedback. In this model we assume that a single remnant galaxy, that forms after the galaxy merger, hosts the MBH pair. The remnant consists of a stellar bulge, stellar disk, and a gas disk.

The radial density of the stellar bulge is described using a power-law profile, truncated at the characteristic outer radius (Binney & Tremaine 2008), and has a total mass proportional to the primary MBH (pMBH) (Magorrian et al. 1998), with the proportionality constant equal to 1000. The stellar and gas disks both follow exponential density profiles (Binney & Tremaine 2008). The temperature profile for the gas disk is calculated using the Toomre stability criterion (Toomre 1964), which gives the minimum temperature for which the gas disk is stable to gravitational collapse. We set the temperature of the disk to be 10^4 K above this minimum temperature, since the interstellar medium after a galactic merger is likely to be shocked and turbulent (e.g., Barnes & Hernquist 1991). Therefore, this gas temperature should be interpreted as a proxy for unmodeled turbulence of warm gas.

Each remnant galaxy is described by five parameters summarized in Table 1. Parameter $M_{\text{bin}} = M_1 + M_2$ is the total mass of the MBH pair and $q = M_2/M_1 < 1$ is the mass ratio of the secondary MBH (sMBH) to the pMBH. $n_{\text{gd}0}$ is the number density of gas particles at the center of the remnant galaxy. Parameter f_{gd} is the gas disk mass fraction defined as $f_{\text{gd}} = M_{\text{gd},1}/(M_{\text{gd},1} + M_{\text{sd},1})$, where $M_{\text{gd},1}$ and $M_{\text{sd},1}$ are the masses of the gas and stellar disks within 1 kpc, respectively. We assume that the gas and stellar disk are rotating with the same speed, $v_{\text{g}}(r)$, while the bulge does not rotate.

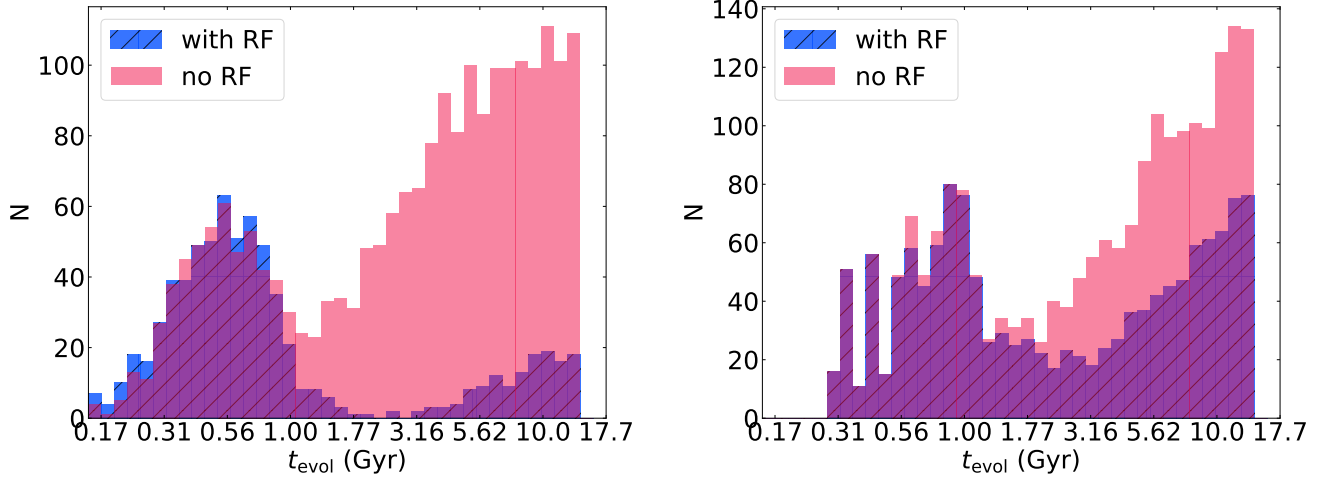


Figure 1. *Left:* Histograms of inspiral time for sMBHs on prograde, low e_i ($e_i < 0.2$) orbits in simulations with and without radiative feedback. *Right:* As in the left-hand panel, but now for sMBHs on retrograde, low e_i orbits. The y -axis in both panels shows the number of MBH pairs with t_{evol} shorter than a Hubble time.

The parameter $v_g(r)$ is in units of circular velocity $v_c(r)$ and $v_g > 0$ indicates that the MBH pair corrotates with the disk and vice versa. The parameter grid shown in Table 1 corresponds to 39366 model galaxies.

We focus on the evolution of unequal mass MBH pairs and fix the location of the pMBH to the center of the remnant. The sMBH orbits the center of the galaxy (and the pMBH) on an orbit that is always coplanar with the galactic disk. We also assume that the sMBH is stripped of its nuclear star cluster in the early stages of the galactic merger preceding the starting point of our simulations. The sMBH is subject to stellar DF exerted by the bulge and stellar disk, and gaseous DF due to the gas disk. We calculate the stellar DF force following equations (5)-(7) in LBB20, based on calculations presented by Antonini & Merritt (2012). The velocity distribution of stars in the bulge is set to be Maxwellian:

$$f(v_*) = \frac{1}{(2\pi\sigma_*^2)^{3/2}} e^{-v_*^2/2\sigma_*^2}, \quad (2)$$

where σ_* is the velocity dispersion of bulge stars, estimated from the $M-\sigma$ relation for the primary MBH (Gültekin et al. 2009; McConnell & Ma 2013).

To evaluate the DF force due to gas, we first use the criteria in equation 1, to determine whether the sMBH is in the regime where gas DF is affected by radiative feedback. If the criteria are not fulfilled, we calculate the gaseous DF force following equations 10–12 in LBB20, corresponding to the case “no RF” below. When the criteria are fulfilled, we use the modified expression for the gaseous DF force shown in the case “with RF”.

$$\vec{F}_{\text{gd}} = -\frac{4\pi(GM_2)^2\rho_{\text{gd}}}{\Delta v^2} \begin{cases} I_R \hat{R} + I_\phi \hat{\phi} & (\text{no RF}), \\ I_R \hat{R} - 0.6I_\phi \hat{\phi} & (\text{with RF}). \end{cases} \quad (3)$$

Here, Δv is the velocity of the sMBH relative to the gas disk and ρ_{gd} is the gas density defined by equation 3 of LBB20. I_R and I_ϕ are the dimensionless components of the DF force in the radial and azimuthal directions, defined by Kim & Kim (2007) and adopted by LBB20. Both I_R and I_ϕ are functions of the Mach number and peak sharply when $\mathcal{M} = 1$. Since commonly $I_\phi \gg I_R$, the gaseous DF force is strongest when Δv is close to the sound speed of the gas.

The key modification in the “with RF” case of equation 3 is motivated by the finding that for a MBH moving through gas on a linear trajectory, the magnitude of the negative DF force is $\sim 60\%$ of that expected without radiative feedback (Park & Bogdanović 2017). We neglect the effect of radiative feedback on the radial component of the DF force, which does not impact the results significantly since $I_\phi \gg I_R$.

Over the course of each simulation, we record the farthest and closest radial distance of the sMBH from the pMBH for every orbit and use them to estimate the orbital semimajor axis (a) and eccentricity (e). Since the galaxy potential is not proportional to $1/r$, and the orbits described by the sMBH are neither Keplerian nor closed, the computed values of a and e are only used to illustrate the shape and size of the orbits. In those terms, the sMBH in each simulation starts on an orbit with $a_i \sim 1$ kpc and initial eccentricity, e_i . The simulations are stopped when the sMBH reaches a separation of 1 pc from the center for the first time.

3. EFFECT OF RADIATIVE FEEDBACK ON THE PAIRING PROBABILITY OF MBHS

Below, we investigate the effect of negative gas DF on the inspiral time (t_{evol}) and pairing probability of MBHs in merger galaxies with different properties. Figure 1 shows histograms of t_{evol} in the scenario where we either account for or neglect radiative feedback. In all cases we calculate t_{evol} as the time for the MBH pair to evolve from an initial

separation of ~ 1 kpc down to 1 pc and the plots show only systems that complete the evolution in less than a Hubble time.

Figure 1(left) illustrates the results for MBHs on prograde orbits with low e_i ($e_i < 0.2$). Without radiation feedback these configurations are characterized by a bimodal distribution of t_{evol} . The left peak of the histogram (at ~ 0.56 Gyr) corresponds to galaxies in which the stellar bulge dominates the orbital evolution of the sMBH, while gaseous DF dominates the evolution for models in the right peak (at ~ 10 Gyr). The difference in the two populations arises because of a significantly larger magnitude of the DF force exerted by the bulge (see § 3.3 in LBB20 for discussion).

In the presence of radiative feedback the distribution of t_{evol} remains bimodal but its right peak is significantly reduced. In comparison, t_{evol} of the MBH pairs whose evolution is dominated by the stellar bulge (the left peak) is only weakly affected. This is because negative DF is more pronounced for MBHs whose orbital evolution is determined by gas. Overall, the number of MBH pairs in prograde, low e_i orbits that reach 1 pc within a Hubble time is reduced from 2170 without radiative feedback to 702 with radiative feedback (a reduction of 67%).

Figure 1(right) shows t_{evol} for sMBHs on retrograde orbits with low e_i . The distribution of t_{evol} is again bimodal, with the left peak corresponding to MBH pairs that evolve due to DF largely exerted by the bulge, and the right peak corresponding to pairs whose evolution is dominated by gaseous DF. For retrograde orbits too, the difference between the two histograms is largest for systems evolving as a consequence of the gas torques. In this case, however, the right peak is not suppressed as severely in the presence of radiative feedback as for the prograde orbits. This is because the sMBHs in retrograde orbits have larger velocities relative to the gas disk, resulting in $\mathcal{M} > 4$ and restored classical gas DF. Consequently, negative DF reduces the number of MBH pairs in retrograde, low e_i orbits that reach 1 pc within a Hubble time from 2083 to 1364 (a reduction of 35%).

We evaluate the magnitude of the DF force for sMBHs on prograde orbits (since, as seen above, these tend to be more affected by negative DF) as a function of two key model parameters: the gas fraction, f_g , and v_g . Here, $f_g = M_{\text{gd}}/(M_{\text{gd}} + M_\star)$ is a parameter that can be compared directly with the gas fraction of galaxies inferred from observations and M_\star includes both the mass of the bulge and stellar disk within the central kiloparsec. LBB20 found that, without radiation feedback, the orbital evolution of MBH pairs in galaxies with $f_g < 0.2$ tends to be dominated by stellar bulges, and in those with $f_g \geq 0.2$ it is dominated by classical gaseous DF.

Figure 2 shows configurations with sMBHs on prograde orbits with low e_i , where each data point corresponds to one simulation. The y-axis of each panel shows the time-averaged azimuthal component of the DF force, F_ϕ , which dominates the orbital evolution and includes contributions from the gas and stellar disk, and stellar bulge. The DF force is in units of $F_{g,0} = 4\pi m_p n_{\text{gd}0} (GM_2/c_s)^2 = 3.7 \times$

10^{31} dyn, evaluated for $n_{\text{gd}0} = 100 \text{ cm}^{-3}$, $M_2 = 10^6 M_\odot$ and $c_s = 10 \text{ km s}^{-1}$. A comparison of the top and bottom left panels in Figure 2 shows a relative dearth of points in simulations with radiative feedback when $f_g \geq 0.1$. These configurations are missing because their t_{evol} becomes longer than a Hubble time. They are the same population of MBH pairs that contribute to the second peak in the histograms of Figure 1 (left panel). Without radiative feedback their t_{evol} is long and comparable to ~ 10 Gyr, because they experience relatively weak DF force ($|\vec{F}_\phi| < 10^{-1} F_{g,0}$). In the presence of radiative feedback, negative DF prevents their gravitational pairing within a Hubble time. Our simulations indicate that, in the presence of negative DF, the pairing probability² of MBHs in near circular prograde orbits in galaxies with $f_g \geq 0.1$ is reduced by 91%, while in galaxies with $f_g < 0.1$ it is only slightly reduced by 1%.

The comparison of the right panels of Figure 2 shows that a significant fraction of MBH pairs on nearly circular prograde orbits with $0.2 < v_g < 0.9$ fail to form bound binaries within a Hubble time in the presence of radiative feedback. This is particularly true for systems experiencing a weaker DF force, $|\vec{F}_\phi| < 10^{-1} F_{g,0}$, characteristic of galaxies where gas DF tends to dominate over stellar DF. This can be understood because the relative velocities of such sMBHs tend to satisfy $\mathcal{M} < 4$, a necessary condition for the onset of negative DF.

Figure 3 is similar to Figure 2 but shows sMBHs in prograde orbits with large e_i ($e_i > 0.8$). The effect of negative DF is now more subtle but still noticeable as a paucity of data points for galaxies with $f_g > 0.1$ (left panels). Collecting all the results from Figs. 2 and 3, we find that negative DF reduces the average pairing probability of MBHs with initially eccentric orbits by 27%, and for those in near circular orbits the probability is reduced by 50%. This difference can be understood by envisioning the action of the DF force in each scenario. The velocity of a prograde sMBH at the apocenter of an eccentric orbit is low relative to that of the gas disk, which classically results in the DF force in the direction of motion, acting to speed up the sMBH and circularize its orbit. In the presence of radiative feedback, however, the DF force reverses direction, decelerating the sMBH and increasing its orbital eccentricity. The inspiral time of such eccentric sMBH is among the shortest in our simulations, since they plunge into the central parsec instead of going through a lengthy inspiral process, like nearly circular sMBHs. These systems appear as the deep blue dots with $|\vec{F}_\phi| < 10^{-2}$ in the right bottom panel of Figure 3. As a result, the pairing probability of MBHs in eccentric prograde orbits is not as severely reduced with radiative feedback compared to MBHs in circular prograde orbits.

Overall, we find that, for the full range of galaxy and MBH properties considered in this work (Table 1) and possible orbital configurations (prograde, retrograde, low/high

² Defined as the fraction of simulations in which the sMBH reaches a separation of 1 pc from the pMBH within a Hubble time.

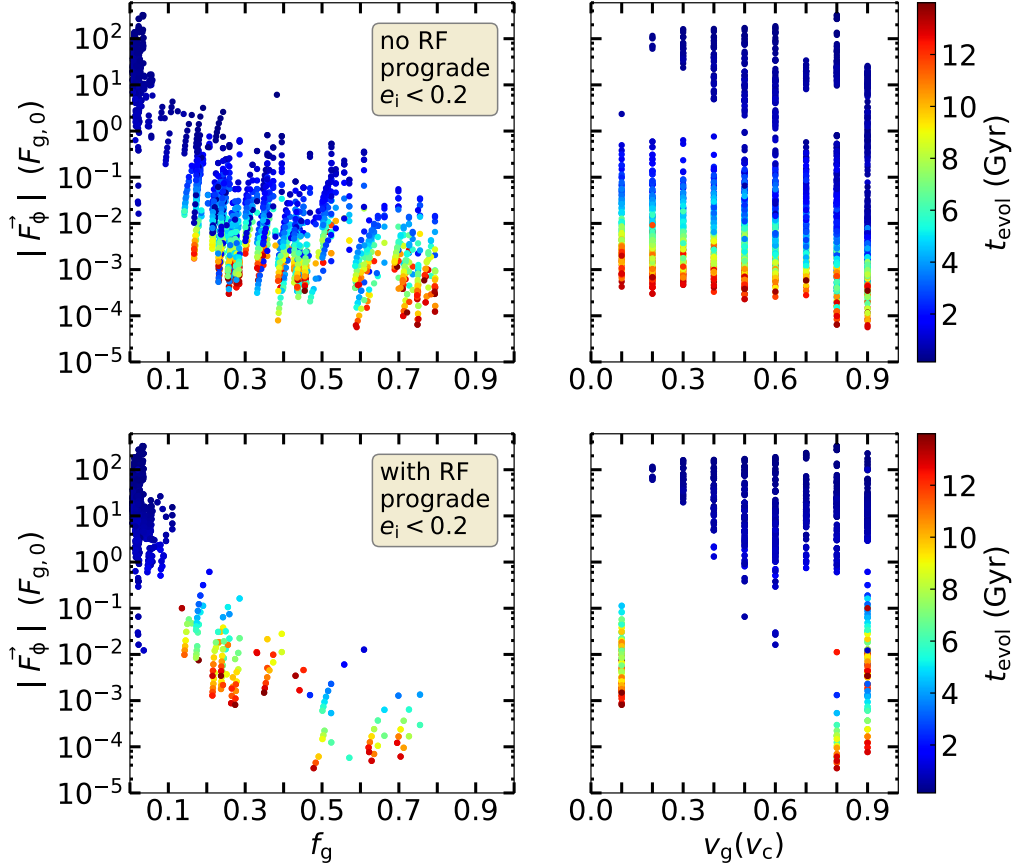


Figure 2. The relationship between the two parameters of the model (f_g and v_g), the total DF force, and the inspiral time (t_{evol}), for MBH pairs with prograde orbits and low initial orbital eccentricity. We show the time averaged azimuthal component of the force, \bar{F}_ϕ , that is responsible for the orbital evolution and neglect the radial component. The top (bottom) row of panels corresponds to simulations without (with) radiative feedback. The color marks the inspiral time. The MBH pairs with inspiral time longer than a Hubble time are not shown in this figure.

e_i), negative DF reduces the MBH pairing probability by 46%. In Figure 4 we collect the results from our entire simulation suite and show this probability as a function of several key parameters in our model. The top left panel shows that radiative feedback reduces the average pairing probability of MBH pairs with total mass in the range of $2 \times 10^5 M_\odot < M_{\text{bin}} < 10^8 M_\odot$ from 0.61 to 0.26 (a reduction of 57%), while the average pairing probability of MBH pairs with masses equal to or larger than $10^8 M_\odot$ is nearly unaffected. This happens because the effect of negative DF, which is more severe for lower mass MBHs (as indicated by the first criterion in equation 1), is compounded with the inefficiency of the DF drag for lower mass objects in general (Park & Bogdanović 2017).

The top right panel of Figure 4 shows that for MBH pairs of all masses the pairing probability increases with q . It nevertheless remains systematically lower by about 35% in simulations that account for the effect of radiative feedback. The

bottom left panel shows that the pairing probability decreases with the galaxy gas fraction. This trend is present in simulations with and without radiative feedback. The difference between the two scenarios is slight in galaxies with $f_g < 0.1$, where the negative DF reduces the average pairing probability by $\sim 7\%$. In galaxies with $f_g \geq 0.1$ however, the average pairing probability is reduced from 0.62 without radiative feedback to 0.19 with radiative feedback (a reduction of $\sim 70\%$). This is consistent with the dependence of the DF force on f_g discussed earlier using the subset of models shown in Figures 2 and 3.

The bottom right panel of Figure 4 illustrates the dependence of the pairing probability on v_g . Without radiative feedback the pairing probability peaks at $v_g = 0.8v_c$ and $v_g = -0.3v_c$. The peak at $v_g = 0.8v_c$ is due to sMBHs in circular orbits that experience efficient gaseous DF. The peak at $v_g = -0.3v_c$ is due to sMBHs in eccentric orbits whose eccentricity continues to increase, resulting in them

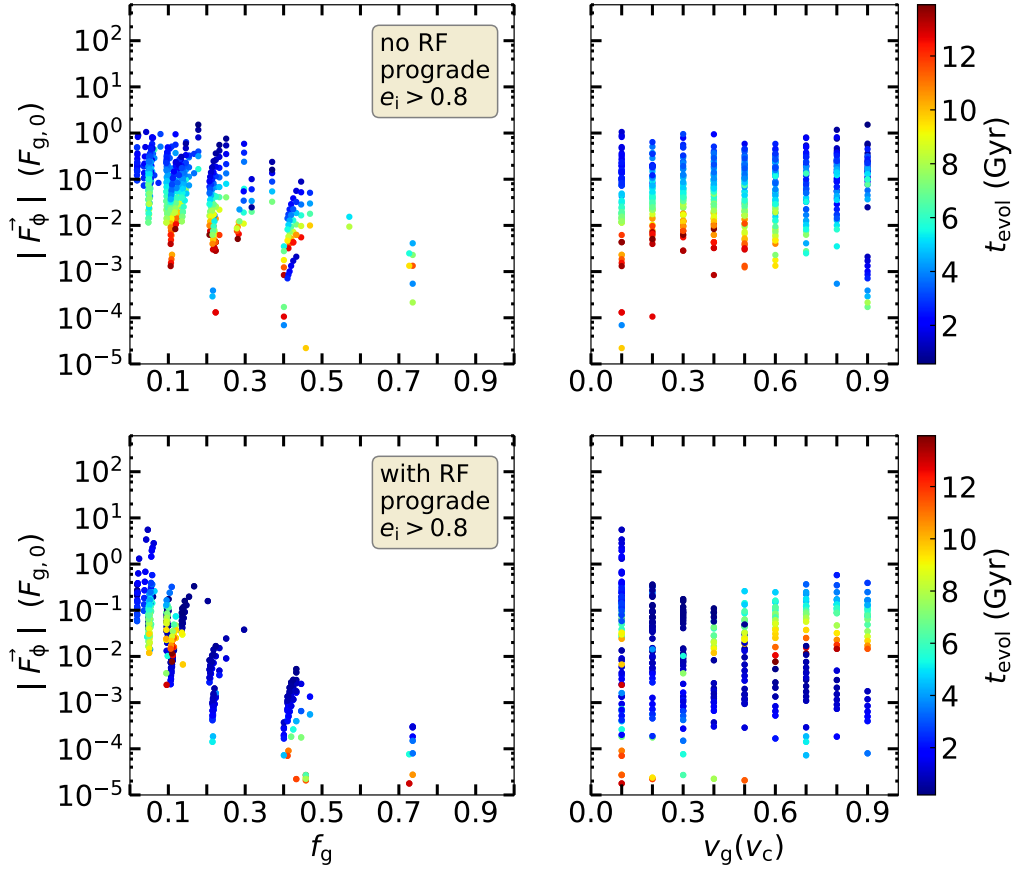


Figure 3. Same as Figure 2 but for MBH pairs in prograde orbits with high initial orbital eccentricity.

plunging into the central parsec. In comparison, in simulations with radiative feedback the pairing is most severely suppressed for prograde MBH pairs in disks with $v_g = 0.8v_c$ and also $v_g = -0.2v_c$, due to the effect of negative DF. Consequently, the average pairing probability of MBH pairs in prograde orbits is reduced from 0.78 without radiative feedback to 0.39 with radiative feedback (a reduction of 50%). For MBH pairs in retrograde orbits, the average pairing probability is reduced from 0.73 without radiative feedback to 0.52 with radiative feedback (a reduction of 28%).

4. POTENTIAL IMPACT OF ASSUMPTIONS

We use a semi-analytic model to evaluate the impact of negative DF on the inspiral time and pairing probability of unequal mass MBH pairs that evolve under the combined influence of stellar and gaseous DF in merger remnant galaxies. The power of using the semi-analytic approach is the ability to compute a large number of simulations of MBH orbital decay, over a wide range of galaxy and MBH properties but at the cost of making some simplifying assumptions. We

summarize the most important assumptions and their impact below and direct the reader to LBB20 for more details.

- The pMBH is fixed at the center of the host galaxy. If the motion of the pMBH was instead captured in our simulations, the resulting inspiral times for the modeled MBH pairs would be shorter, particularly in systems with comparable mass MBHs.
- The mass of the two MBHs is assumed to remain constant during the inspiral, even in galaxies with substantial gas fractions. Accretion onto the MBHs during inspiral may change their mass ratio and impact the properties of the evolution. While the exact impact depends on the details of the accretion onto the MBHs (e.g., Siwek et al. 2020), an increase in the total mass of the MBH pair will result in a shorter inspiral time.
- The sMBH is assumed to be completely stripped of its remnant stellar cluster during our simulations. This is a plausible outcome for our starting radius of ≈ 1 kpc (Kelley et al. 2017b). If some portion of the stellar

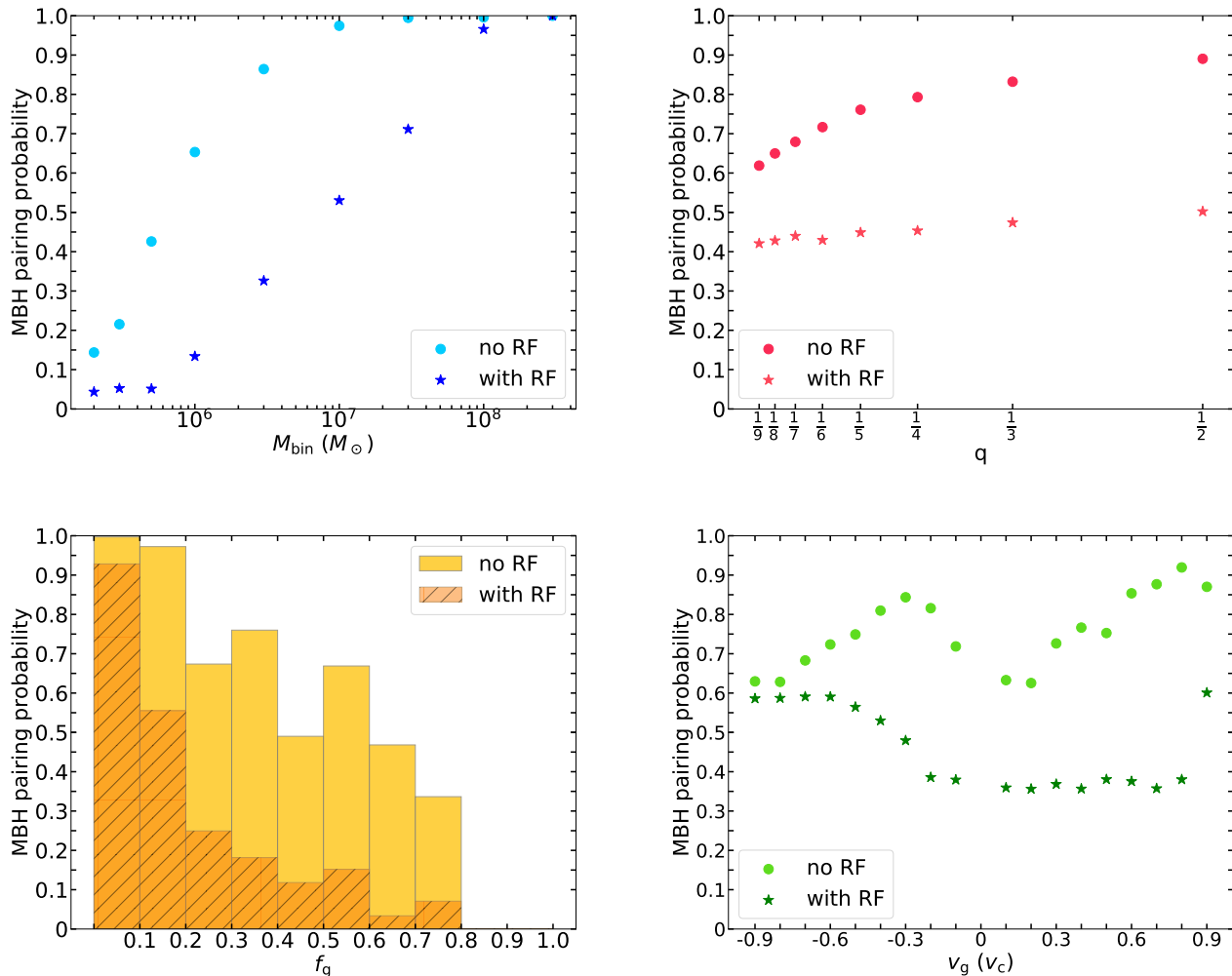


Figure 4. MBH pairing probability as a function of the host galaxy and MBH pair properties with and without radiative feedback: M_{bin} (top left), q (top right), f_g (bottom left), and v_g (bottom right). We show the dependence on f_g as a histogram, since this is a derived, rather than a primary parameter with assumed equidistant values.

cluster survives until late into the inspiral, it would lead to more efficient DF and a shorter orbital evolution time of the MBH pair (Dosopoulou & Antonini 2017).

- The orbit of the sMBH is assumed to be co-planar with the galactic gas and stellar disks. It is nevertheless possible that some fraction of sMBHs evolve on orbits that are inclined relative to the galactic disk. sMBHs on inclined orbits on the one hand experience weaker DF from the gas and stellar disks, an effect that leads to longer inspiral times. On the other hand, perturbations triggered by pericentric passages of the sMBH crossing the disk of the remnant galaxy can trigger the formation of a dense stellar cusp around the sMBH. This effect leads to the increase of stellar mass bound to the sMBH and can shorten the orbital evolution time (Van Wassenhove et al. 2014).

- The gas disk in our model is smooth and devoid of spiral arms or gas clumps. When they are present, interactions between the sMBH and these structures can lead to a random walk of the sMBH, resulting in longer orbital evolution time. In some cases, when the inhomogeneities are large enough, the sMBH may even be ejected out of the galactic disk (Tamburello et al. 2017).

5. CONCLUSIONS

We find that, for a wide range of galaxy and MBH properties, negative DF reduces the MBH pairing probability by 46%. In addition, we find that:

- The effect of negative DF is most pronounced in galaxies with significant gas fractions, where gas DF determines orbital evolution of the MBH pairs. For example, in galaxies with $f_g \geq 0.1$ negative DF results in longer MBH inspiral times and reduces the pairing

probability by 70%. In contrast, the pairing probability is only slightly reduced in galaxies with $f_g < 0.1$, in which MBH pairs mostly evolve under the influence of stellar DF.

- Negative DF has a stronger impact on MBHs in prograde orbits (as opposed to those in retrograde orbits), since their Mach numbers are more likely to have values $\mathcal{M} < 4$ and fulfill a necessary criterion for the onset of negative DF. Similarly, MBH pairs in low e_i orbits are more significantly affected by negative DF than those in large e_i orbits. This happens because negative DF tends to promote eccentricity growth of already eccentric orbits. The inspiral time of such eccentric MBHs is among the shortest in our simulations, since they plunge into the central parsec instead of going through the lengthy inspiral process.
- We find that negative DF reduces the pairing probability of MBH pairs with total mass $< 10^8 M_\odot$ by 57%. The effect of negative DF, which is more severe at the lower mass end of the MBH spectrum, is compounded with the inefficiency of the DF drag for

lower mass objects in general. This is of importance because MBH pairs in this mass range are expected to be direct progenitors of merging binaries targeted by the future space-based GW observatory LISA. Specifically, if negative DF operates as described here, the merger rates of MBHBs detectable by LISA may be substantially reduced.

Overall, we conclude that negative DF generated by the ionizing radiation produced by the inspiralling sMBH is a potentially important dynamical effect on the evolution of MBH pairs in post-merger galaxies. Future numerical investigations of the formation of MBHBs should consider the influence of negative DF, in particular in gas-rich galaxies with pair masses $< 10^8 M_\odot$.

ACKNOWLEDGMENTS

T.B. acknowledges the support by the National Aeronautics and Space Administration (NASA) under award No. 80NSSC19K0319 and by the National Science Foundation (NSF) under award No. 1908042. The authors thank Fabio Antonini for helpful comments.

REFERENCES

- Amaro-Seoane, P., Audley, H., Babak, S., et al. 2017, arXiv e-prints, arXiv:1702.00786
- Antonini, F., & Merritt, D. 2012, *ApJ*, 745, 83
- Arzoumanian, Z., Baker, P. T., Brazier, A., et al. 2018, *ApJ*, 859, 47
- Barausse, E. 2012, *MNRAS*, 423, 2533
- Barnes, J. E., & Hernquist, L. E. 1991, *ApJL*, 370, L65
- Begelman, M. C., Blandford, R. D., & Rees, M. J. 1980, *Nature*, 287, 307
- Berczik, P., Merritt, D., Spurzem, R., & Bischof, H.-P. 2006, *ApJL*, 642, L21
- Berti, E., Sesana, A., Barausse, E., Cardoso, V., & Belczynski, K. 2016, *PhRvL*, 117, 101102
- Binney, J., & Tremaine, S. 2008, *Galactic Dynamics: Second Edition* (Princeton University Press)
- Chandrasekhar, S. 1943, *ApJ*, 97, 255
- Cuadra, J., Armitage, P. J., Alexander, R. D., & Begelman, M. C. 2009, *MNRAS*, 393, 1423
- Dosopoulou, F., & Antonini, F. 2017, *ApJ*, 840, 31
- Dotti, M., Colpi, M., Haardt, F., & Mayer, L. 2007, *MNRAS*, 379, 956
- Escala, A., Larson, R. B., Coppi, P. S., & Mardones, D. 2005, *ApJ*, 630, 152
- Foster, R. S., & Backer, D. C. 1990, *ApJ*, 361, 300
- Gruzinov, A., Levin, Y., & Matzner, C. D. 2020, *MNRAS*, 492, 2755
- Gültekin, K., Richstone, D. O., Gebhardt, K., et al. 2009, *ApJ*, 698, 198
- Inayoshi, K., Haiman, Z., & Ostriker, J. P. 2016, *MNRAS*, 459, 3738
- Kelley, L. Z., Blecha, L., & Hernquist, L. 2017a, *MNRAS*, 464, 3131
- . 2017b, *MNRAS*, 464, 3131
- Kelley, L. Z., Blecha, L., Hernquist, L., Sesana, A., & Taylor, S. R. 2017c, *MNRAS*, 471, 4508
- Khan, F. M., Holley-Bockelmann, K., Berczik, P., & Just, A. 2013, *ApJ*, 773, 100
- Khan, F. M., Just, A., & Merritt, D. 2011, *ApJ*, 732, 89
- Kim, H., & Kim, W.-T. 2007, *ApJ*, 665, 432
- Klein, A., Barausse, E., Sesana, A., et al. 2016a, *PhRvD*, 93, 024003
- . 2016b, *PhRvD*, 93, 024003
- Kormendy, J., & Richstone, D. 1995, *ARA&A*, 33, 581
- Lentati, L., Taylor, S. R., Mingarelli, C. M. F., et al. 2015, *MNRAS*, 453, 2576
- Li, K., Bogdanović, T., & Ballantyne, D. R. 2020, *ApJ*, 896, 113 (LBB20)
- Magorrian, J., Tremaine, S., Richstone, D., et al. 1998, *AJ*, 115, 2285
- McConnell, N. J., & Ma, C.-P. 2013, *ApJ*, 764, 184
- Ostriker, E. C. 1999, *ApJ*, 513, 252
- Park, K., & Bogdanović, T. 2017, *ApJ*, 838, 103

- Park, K., & Ricotti, M. 2013, *ApJ*, 767, 163
- Quinlan, G. D. 1996, *NewA*, 1, 35
- Quinlan, G. D., & Hernquist, L. 1997, *NewA*, 2, 533
- Shannon, R. M., Ravi, V., Lentati, L. T., et al. 2015, *Science*, 349, 1522
- Siwek, M. S., Kelley, L. Z., & Hernquist, L. 2020, *MNRAS*, 498, 537
- Soltan, A. 1982, *MNRAS*, 200, 115
- Tamburello, V., Capelo, P. R., Mayer, L., Bellovary, J. M., & Wadsley, J. W. 2017, *MNRAS*, 464, 2952
- Toomre, A. 1964, *ApJ*, 139, 1217
- Toyouchi, D., Hosokawa, T., Sugimura, K., & Kuiper, R. 2020, *MNRAS*, arXiv:2002.08017
- Van Wassenhove, S., Capelo, P. R., Volonteri, M., et al. 2014, *MNRAS*, 439, 474
- Yu, Q. 2002, *MNRAS*, 331, 935